Evaluation of MRI-based measurement for quantifying prostate development in mice with prostate-specific PTEN deletion

J. Tsao[1], G. Boynton[1], M. Privetera[1], and C. Timmers[1]
[1]Novartis Institutes for BioMedical Research, Inc., Cambridge, MA, United States

Introduction

PTEN (phosphatase and tensin homolog deleted on chromosome 10) is centrally involved in the development of human prostate cancer. Thus, mouse models of prostate-specific PTEN deletion (1) serve as important tools to study tumor development and to evaluate the efficacy of anti-tumor compounds targeting the PTEN / PI3-K / AKT pathway (PI3-K = phosphoinositide 3-kinase, AKT = protein kinase B). In the context of preclinical research, the internal position of the prostate makes it difficult to evaluate tumor progression with conventional, non-imaging means. Previously, MRI has been applied to quantify prostate development [2-4]. So far, most of the reported quantitation has been limited to a small number of animals and examining large changes between wildtypes and mutant strains. The purpose of this study was to establish the accuracy and sensitivity of an MRI-based method to detect subtle changes in prostate volume. Specifically, image segmentation and analysis methods were developed to allow accurate and reproducible determination, which opens up the possibility of quantifying treatment efficacy in genetic models that may be more representative of the natural settings in the human disease.

Methods and Materials

Animals Male mice (age 12-17 weeks, 20-35g) from two models of prostate-specific PTEN deletion were used ($Pten^{f/f}$:$PbCre^{+}$ and $Pten^{f/-}$:$PbCre^{+}$). Mice from the first line ($Pten^{f/f}$:$PbCre^{+}$) develop prostatic intraepithelial neoplasia (PIN) by 9 weeks of age but rarely progress to adenocarcinoma. In the second more aggressive line ($Pten^{f/-}$:$PbCre^{+}$), one of the *Pten* alleles is deleted, so the animals are heterozygous for *Pten* throughout the body except for the prostate epithelium which is completely deleted for *Pten*. This line progresses to PIN at a faster rate and the mice develop invasive carcinoma as early as 15 weeks of age.

MRI and image analysis Axial and coronal MR images were acquired on a Bruker 4.7T PharmaScan MRI (Bruker BioSpin, Ettlingen, Germany) using a T_2-weighted fast-spin echo sequence with TE/TR = 42/4061ms, a voxel size of 0.15x0.20x0.60mm^3, and a scan time of 6min30s. Axial images were segmented using an inhouse-modified version of the ITK-SNAP software (5). In both models ($PTEN^{f/f}$ and $PTEN^{f/-}$) the anterior lobes of the prostate often became cystic. Thus, the delineated region underwent automatic classification to differentiate cystic and non-cystic tissues (Fig. 1). The segmentation algorithm involved a histogram analysis for intensity calibration, and a combination of thresholding, watershed, and connectivity criteria for segmentation. Adjustable parameters for the algorithm were chosen from a subset of images (4 datasets), and the same parameters were used reliably across all animals. Shape-based interpolation was used to improve 3D visualization of the segmented volumes. To estimate measurement reproducibility, 11 mice (3 $PTEN^{f/f}$ and 8 $PTEN^{f/-}$) were imaged twice on the same day and analyzed separately. To estimate accuracy, 20 mice (11 $PTEN^{f/f}$ and 9 $PTEN^{f/-}$) were imaged prior to tissue harvest and *ex vivo* wet weight measurement. All experiments were conducted in accordance to institutionally approved protocols.

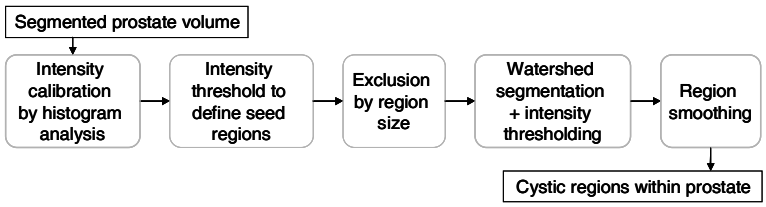

Fig. 1. Schematic of tissue classification algorithm

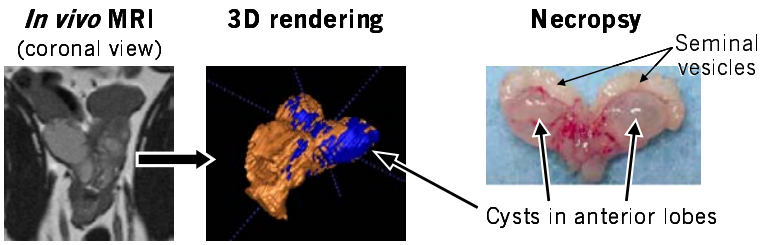

Fig. 2. 3D visualization of prostate by MRI compared to necropsy

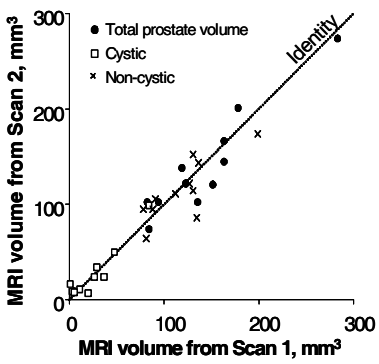

Fig 3. Reproducibility from scan-rescan comparison

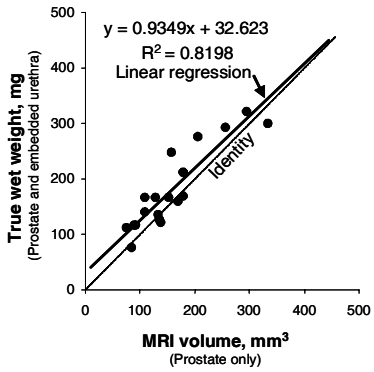

Fig 4. Accuracy compared to *ex vivo* wet weight

Results

Fig. 2 shows a representative coronal MR image of the prostate, a shape-based-interpolated 3D rendering of the segmented and classified regions of the prostate, and a photograph of the excised prostate with seminar vesicles attached at the top.

Fig. 3 shows the correlation between repeated scans of the same animals for the total prostate volume, and the classified cystic and non-cystic portions. Bland-Altman analysis (7) of the data yielded standard deviations of 19.7mm^3, 9.4mm^3, and 20.9mm^3 for the total, cystic and non-cystic prostate volumes, respectively. Fig. 4 shows the correlation between the *ex vivo* wet weight and the total prostate volume measured by MRI with an R^2 of 0.82.

Power analysis Based on the estimated variability from the repeated measurements, the sensitivity for detecting treatment effects could be estimated by power analysis. For this purpose, it was assumed that a 2-tailed unpaired t-test would be used to compare two groups of equal size N, and that the intra-group variability was unaffected by treatments. In that case, for a representative group size of N = 8, the minimum changes detectable by MRI (i.e. minimum treatment effects) are 27.3mm^3, 13.0mm^3, and 29.0mm^3 for the total, cystic and non-cystic prostate volumes, respectively.

Discussion

This work quantified the reliability of *in vivo* MRI-based measurement of the total, cystic and non-cystic prostate volumes in the mouse. The accuracy and reproducibility of the measurements were evaluated respectively by comparison with *ex vivo* wet weights and repeated scans of the same animals on the same day. The results show the capability of MRI-based measurements to detect subtle changes in prostate volume in the mouse that opens up the possibility for longitudinal quantitation of the efficacy of therapeutic agents.

References

1. Wang S et al. Cancer Cell, 4, 209-21. 2003. 2. Song SK et al. Cancer Res, 62, 1555-8. 2002. 3. Trotman LC et al. PLoS Biol, 1, E59. 2003. 4. Fricke ST et al. Prostate, 66, 708-17. 2006. 5. Yushkevich PA et al. Neuroimage, 31, 1116-28. 2006. 6. Raya S, Udupa J. IEEE TMI. 9:33-42. 1990. 7. Bland JM & Altman DG, Lancet, 1, 307-10. 1986.